JOURNAL OF MATERIALS SCIENCE 28 (1993) 4483–4488

The high-temperature creep behaviour of an Al–1 wt% Cu solid-solution alloy

M. S. SOLIMAN
Mechanical Engineering Department, College of Engineering, King Saud University, P.O. Box 800, Riyadh 11421, Saudi Arabia

The creep behaviour of an Al–1 wt% Cu solid-solution alloy is investigated at a temperature of 813 K under stress range of 0.5–5 MPa. The creep characteristics of the alloy including the stress dependence of the steady-state creep rate ($n = 4.4$), the shape of creep curve (normal primary stage), the transient creep after stress increase, and the value of the true activation energy for creep, suggest that some form of dislocation climb is the rate-controlling process at higher stresses above 1 MPa. However, at low stresses (< 1 MPa), the creep curves show no distinguished steady state, and the stress dependence of the minimum creep rate is as high as ~ 8. The creep behaviour of the alloy is discussed based on recent theories available for describing creep in solid-solution alloys.

1. Introduction

It is well established at high temperatures and intermediate stresses in the range ($10^{-5}G < \sigma < 10^{-3}G$), where σ is the stress and G is the shear modulus, that the stress dependence of the steady-state creep rate, $\dot{\varepsilon}$, of pure metals and solid-solution alloys can be represented by the creep power-law [1, 2] of the form

$$\dot{\varepsilon} = A\left(\frac{DGb}{kT}\right)\left(\frac{\sigma}{G}\right)^n \quad (1)$$

where A is a constant, b is Burgers vector, D is the diffusion coefficient, kT is the Boltzmann constant times the absolute temperature, and n is the stress exponent. The value of n for pure metals is close to 5. However, two limiting values for solid solutions have been reported: the upper limiting value is essentially similar to that observed in pure metals ($n \simeq 5$), while the lower limiting value is ~ 3. Based on the value of n and other creep characteristics, the solid-solution alloys have been divided into two groups [3, 4]: the "alloy" class (Class I) and the "pure metal" class (Class II). It is believed that some form of dislocation climb is the rate-controlling process in pure metals and metal-class alloys [2, 5], while viscous glide motion of dislocations dragging the solute atmosphere is the rate-controlling process in alloy-class alloys [6, 7].

It is suggested [2, 7, 8] that both dislocation climb and viscous glide are operating in a sequential manner in any solid-solution alloy and the slower process controls the creep behaviour. Based on this suggestion, it has been shown [4, 8] that transition from viscous glide ($n = 3$) to dislocation climb ($n = 5$) may take place in a single alloy when the applied stress is decreased below a critical value. This expectation has been verified experimentally in a number of investigations on aluminium alloys [9–15] and other alloy systems [16–20]. The transition in the value of stress exponent from $n \sim 3$ at high stresses to $n \sim 5$ at low stresses in Al–Mg alloys [13, 14] has been accompanied by a substructural change in accordance with the change in the creep mechanism from viscous glide to dislocation climb. The substructure has changed from a uniform distribution of dislocations at high stresses to well-developed sub-boundaries at low stresses.

The transitions in the creep behaviour reported recently for dilute Al–Mg alloys [21–23] containing 0.5–3 at % Mg and that for Al–0.86 at % Cu [24] and Al–1.3 at % Cu [25], have motivated the present investigation. An aluminium alloy containing 0.47 at % Cu was selected and the present paper reports the experimental results obtained for this alloy.

2. Experimental procedure

The alloy of Al–1.1 wt% Cu (Al–0.47 at % Cu) was prepared by melting aluminium and copper of 99.99% purity. It was supplied in the form of hot-rolled strips, 3 mm thick.

Tensile specimens of 25 mm gauge length and 12.5×3 mm^2 cross-section were machined from the strip such that the tensile axis was parallel to the rolling direction. The specimens were hand polished and prior to testing, all specimens were annealed *in situ* for 2 h at 843 K to remove the effects of machining and to produce a stable uniform grain size. The produced grain size, as measured by a procedure based on deformation by grain-boundary sliding [15], was ~ 2 mm. After annealing, specimens were cooled to the testing temperature of 813 K (0.9 T_m, where T_m is the melting point of the alloy).

Creep experiments were conducted on a Mayes electronic creep testing machine which keeps the stress constant, based on the principle of constant volume of

0022–2461

the specimen, up to strain of 0.2. During the test, as the specimen stretches uniformly under constant stress control, the load will be uniformly reduced. All the mechanical tests were conducted in air in a three-zone furnace and temperatures were monitored with three Pt/Pt–13% Rh thermocouples held in direct contact with the middle of the gauge length and the grips of the specimens. The testing temperature was stabilized and maintained to within $\pm$ 1 K of the reported temperature. The room temperature was stabilized to within $\pm$ 2 K. The strain during creep was measured with two capacitance transducers, connected to the extensometer outside the heating zone, and whose outputs were averaged out and monitored directly on a strip chart recorder. Sufficient strain was attained in each test to establish unequivocally the steady-state creep. The stress-increase experiments were conducted by rapidly increasing the static command of stress. The activation energy was measured by conducting creep tests at different temperatures for the same applied stress.

The creep curves were plotted using a spread sheet and a PC microcomputer.

3. Experimental results

3.1. Creep curves

The creep curves of the alloy at high stresses showed a pronounced region of normal primary creep where the creep rate continuously decreased until the steady state was reached after strain $\leqslant 10\%$, as shown in Fig. 1. The amount of instantaneous strain upon load application was small and the primary strain increased with the applied stress. At low stresses (< 1 MPa), no instantaneous strain was observed and the creep rate increased with strain over a short period of time and the creep curve thereafter showed the characteristics of dynamic recrystallization and no distinguishable steady state was observed; see for example, the creep curve at $\sigma = 0.5$ MPa as plotted in Fig. 2. For such low stress the creep experiment was conducted for more than 1000 h. Also, Fig. 2 shows the calculated strain rate as a function of time/strain. Because no steady state was observed at low stresses, the minimum creep rate was used to study the stress dependence of the creep rate.

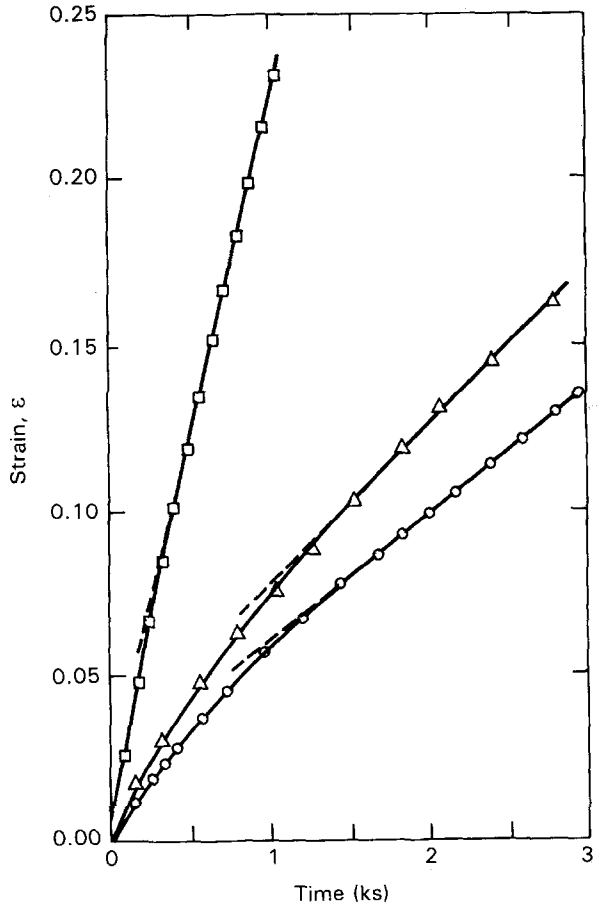

Figure 1 Typical examples for creep curves of Al–1 wt% Cu at high stresses. $T = 813$ K, σ: (□) 2.7 MPa, (△) 2.1 MPa; $T = 773$ K, (○) $\sigma = 2.5$ MPa.

3.2. Stress dependence of the steady-state creep rate

Experimental data representing the stress dependence of the steady state creep rate are shown in Fig. 3, where steady state creep rate, $\dot{\varepsilon}$, is plotted versus the applied stress, σ, on a logarithmic scale for the testing temperature 813 K. As mentioned earlier, at stresses below 1 MPa, the steady state is represented by the minimum creep rate. The creep data, presented in Fig. 3, obey the creep power law, with a stress exponent, n, of 4.4 at high stresses which increases to a value of 8.2 at low stresses. The creep data for pure aluminium [2], as represented by a dotted line having a slope of 4.5, are also included in Fig. 3 for the purpose of comparison; the creep rate for pure aluminium at 813 K is calculated using Equation 1. The value of stress exponent for the alloy at high stresses is very close to the value of $n = 4.5$ reported for pure aluminium [2]. However, examination of Fig. 3, reveals two points: (i) the addition of 1 wt% Cu to aluminium decreases the creep rate by more than one order of magnitude for the same stress, (ii) the stress exponent in the alloy increases to a higher value at low stresses (< 1 MPa).

3.3. Activation energy for creep

Creep experiments at constant stress ($\sigma = 2.5$ MPa),

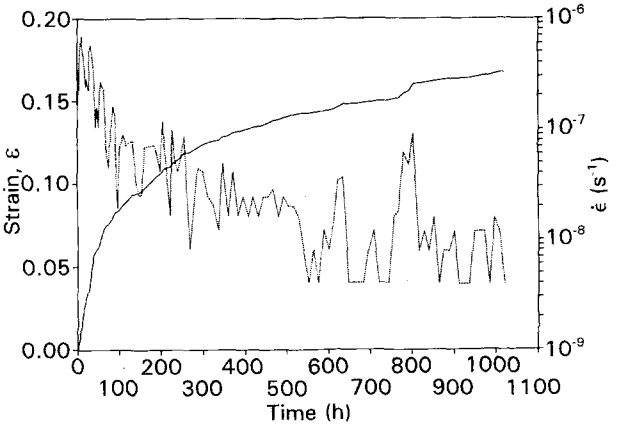

Figure 2 (——) A creep curve for Al–1 wt% Cu at $\sigma = 0.5$ MPa and $T = 813$ K. Also, included is the creep rate, $\dot{\varepsilon}$ (···) as a function of strain/time.

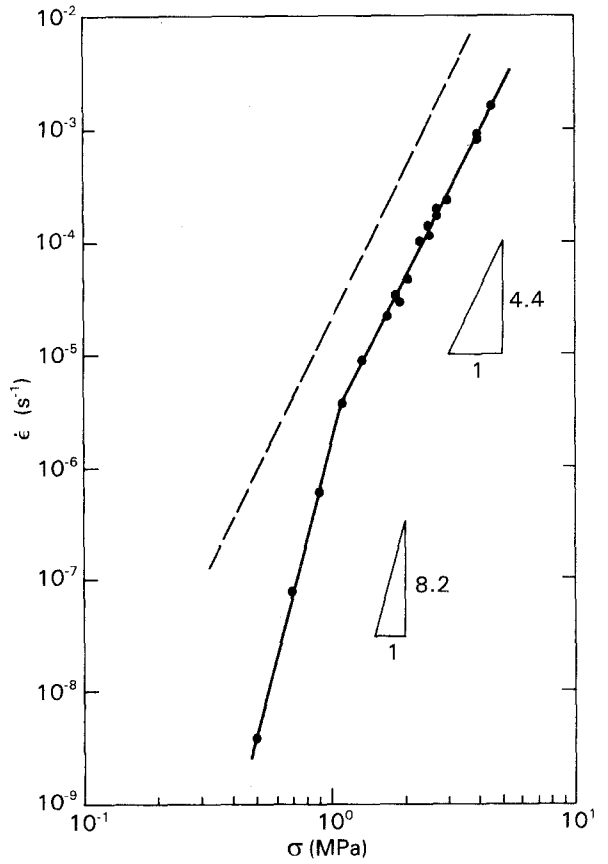

Figure 3 The stress dependence of the steady-state creep rate at high stresses and the minimum creep rate at low stresses (< 1 MPa) for Al–1 wt% Cu at $T = 813$ K.

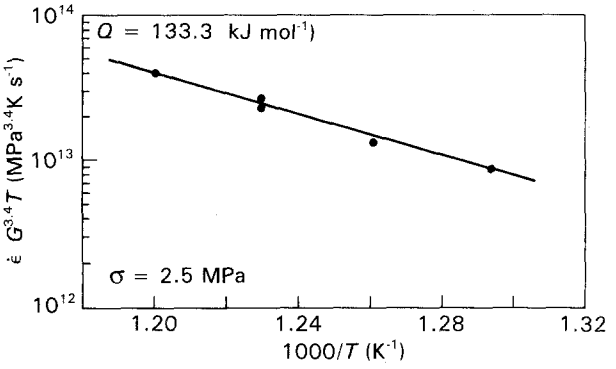

Figure 4 Determination of the true activation energy for creep in Al–1 wt% Cu at high stresses by plotting $\dot{\epsilon}G^{3.4}T$ versus $1/T$ at $\sigma = 2.5$ MPa.

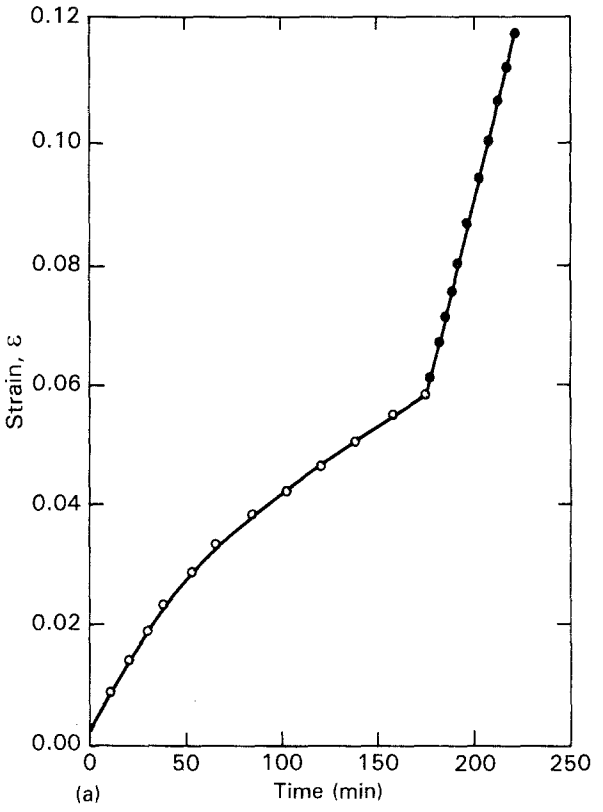

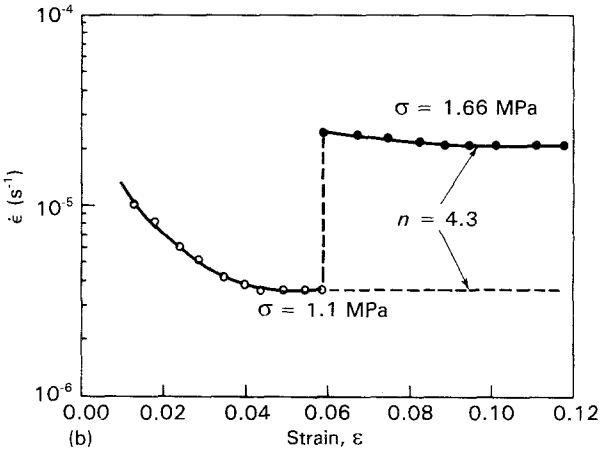

Figure 5(a) An example for stress increase experiment from (○) $\sigma_1 = 1.1$ MPa to (●) $\sigma_2 = 1.66$ MPa showing the transient strain as a function of time. (b) Strain rate, $\dot{\epsilon}$, versus strain, ϵ, for the stress increase experiment shown in (a). The two solid arrows indicate the strain rates used to calculate the stress exponent $n = \ln(\dot{\epsilon}_2/\dot{\epsilon}_1)/\ln(\sigma_2/\sigma_1)$.

were carried out at different temperatures; the creep curves obtained are similar to those obtained at $T = 813$ K (see Fig. 1). The steady-state creep rates of these experiments are plotted in Fig. 4 as $\log(\dot{\epsilon}G^{3.4}T)$ versus $1/T$; the data points fall very close to a straight line. The true activation energy inferred from the slope of the straight line is $Q = 133$ kJ mol^{-1}. This value is very close to the aluminium self-diffusion coefficient [26]. Because of dynamic recrystallization, no attempt was made to determine the activation energy at low stresses.

3.4. Stress-increase experiment

Stress-increase experiments were performed at high stresses. An example is shown in Fig. 5a and b for a stress increase from $\sigma_1 = 1.1$ MPa to $\sigma_2 = 1.66$ MPa. Fig. 5a illustrates the creep strain with time and indicates that no instantaneous strain has occurred after the stress increase. Fig. 5b shows the strain rate, $\dot{\epsilon}$, versus creep strain and examination of this figure reveals the following: (i) a stress increase to σ_2 has occurred after reaching the steady state at σ_1, (ii) initial creep rate after a stress increase from σ_1 to σ_2 is higher than the new steady state at σ_2, and (iii) the stress exponent estimated from stress-increase experiment is in good agreement with that obtained from steady-state creep data as plotted in Fig. 3. These results are consistent with those obtained for pure

aluminium [27, 28] and Al–5% Zn [29] at high temperatures.

4. Discussion

4.1. Creep mechanism in the alloy

The present results on Al–1 wt% Cu at high stresses, including the value of stress exponent ($n = 4.4$), the shape of transient creep after stress application or stress increase, and the value of true activation energy for creep, suggest that dislocation climb [2, 5] is the rate-controlling process under the present experimental conditions. However, examination of Fig. 3, shows that the addition of 1 wt% Cu to aluminium has modified the deformation process in two ways. First, the creep rate of the alloy is about one order of magnitude slower than pure aluminium. Second, the stress exponent of the alloy increases with decreasing the applied stress.

Recently, Argon and Takeuchi [30] have developed a theory to explain the creep behaviour of pure metals and metal-class alloys. They assumed that the creep deformation is not driven by the applied stress, but rather by an effective stress; $\sigma_e = \sigma - \sigma_i$, where σ_i is the internal stress. The authors assumed that the exclusive source of internal stress in the steady-state creep of subgrain-forming alloys is the bowing of subboundaries of such subgrains under the action of the applied stress. They found that the internal stress, σ_i, can be given by the equation

$$\sigma_i/G = \frac{\alpha(1-\nu)}{\pi}(K\theta)^{1/3}(\sigma/G)^{2/3} \quad (2)$$

where $\alpha = 0.317$, $K = 30$, ν is Poisson's ratio (= 0.33) and θ is the misorientation angle between subgrains (= 1°). The values of (σ_i/G) obtained from Equation 2 were in reasonable agreement with the experimental values of internal stresses measured by the stress-dip technique, in pure metals and metal-class alloys. Consequently, Argon and Takeuchi have written the creep rate in pure metals and metal-class alloys as

$$\dot{\varepsilon} = A'\frac{DG\boldsymbol{b}}{kT}\left(\frac{\Gamma}{G\boldsymbol{b}}\right)^3\left[\frac{\sigma}{G} - \frac{\alpha(1-\nu)}{\pi}(K\theta)^{1/3}(\sigma/G)^{2/3}\right]^3 \quad (3)$$

where A' is a dimensionless constant, Γ is the stacking fault energy. This equation is similar to that developed previously [2, 4], except for the internal stress term (Equation 2) and the stress exponent. Equation 3 has an interesting feature: the stress exponent ($n = \partial\ln\dot{\varepsilon}/\partial\ln\sigma$) increases with decreasing applied stress due to the increase in the ratio of σ_i/σ at lower stresses [30, 31]. Therefore, the increase in the importance of internal stress may explain the increase in n with decreasing applied stress for the present alloy. However, Equation 2 predicts internal stresses higher than the applied stresses at stresses below $\sigma/G < 2 \times 10^{-4}$. Therefore, Equation 2 cannot be applied quantitatively to predict the behaviour of Al–1 wt% Cu which was crept at stresses below $2 \times 10^{-4}G$. Instead, the semi-empirical equation developed for dislocation climb-controlled creep [4] will be used as shown in the next section. It is worth mentioning that dynamic recrystallization was reported to occur during the high-temperature creep of Ni–W dilute solid-solution alloys [32]. A stress exponent as high as 7.2 was reported for Ni–5 wt% W [33]; however, for Ni–1 wt% W [32], the stress dependence of the minimum creep rate was not determined. Under steady-state conditions (no dynamic recrystallization), the stress exponent for other Ni–W alloys was very close to 5 [32].

4.2. Prediction of the creep behaviour of a solid-solution alloy

Attempts have been made to predict the class of behaviour of a solid-solution alloy. First, it was suggested [8] that viscous glide ($n = 3$) is a controlling process in alloys with large misfit parameter, e, while dislocation climb is rate-controlling in alloys with high shear modulus. Later, a deformation criterion [4] was developed, based on the suggestion [2, 7, 8] that both viscous glide and dislocation climb are sequential processes in solid solutions (the slower controls the creep behaviour), and the viscous glide process solely results from the Cottrell–Jaswon interaction mechanism [34]. The criterion is written [4] in the form

$$\left(\frac{1}{X_B}\right)\left(\frac{kT}{eG\boldsymbol{b}^3}\right)^2 = B\left(\frac{\Gamma}{G\boldsymbol{b}}\right)^3(D_c/D_g)(\sigma/G)^2 \quad (4)$$

where X_B is the solute concentration, D_c is climb diffusion coefficient, D_g is the glide diffusion coefficient and B is a constant. In addition to the prediction of the class of behaviour of an alloy, the criterion shows that transition from viscous glide at high stresses to dislocation climb at low stresses can take place in a single alloy, provided that the condition given by Equation 4 is satisfied. The modifications introduced to Equation 4 by incorporating the contributions of other viscous drag processes [35], will not be considered here, as it has been shown [35] that the Cottrell–Jaswon mechanism [34] is responsible for the viscous glide process in Al–Cu and Al–Mg alloys.

Application of Equation 4 to predict the class of behaviour of an alloy, requires proper values for D_c, D_g, $(\Gamma/G\boldsymbol{b})$ and the constant B. Recent theoretical analysis [36] and experimental studies [15, 20, 35, 37–39] have shown that the appropriate values of D_c and D_g are given by the following expressions, respectively

$$D_c = (X_A D_A + X_B D_B)/f \quad (5)$$

$$D_g = \frac{D_A D_B \phi}{(X_A D_A + X_B D_B)} \quad (6)$$

where D_A, D_B are the self-diffusion coefficient of A and B, X_A and X_B are their respective atomic fraction in the alloy A–B, f a correlation factor close to unity, and ϕ is the thermodynamic factor. In the absence of experimental data for stacking fault energy in most solid-solution systems, a procedure will be developed to evaluate this parameter $(\Gamma/G\boldsymbol{b})$. Because it was shown that the creep rates of pure metals and metal-class alloys are dependent on stacking fault energy [2,

32, 40, 41], the creep rate under dislocation climb control [4] is written as

$$\dot{\varepsilon}_c = A_c \frac{D_c G b}{kT}\left(\frac{\Gamma}{Gb}\right)^3 (\sigma/G)^5 \qquad (7)$$

where A_c is a constant. Using Equation 5 for D_c, the normalized parameter $(\dot{\varepsilon}kT/D_cGb)/(\sigma/G)^5$ is plotted versus (Γ/Gb) for a number of pure metals and metal-class alloys [2, 4, 37, 42] as shown in Fig. 6. The data points for the alloys and pure metals coalesce on a straight line having a slope of ~ 3 (3.15). The dependence of creep rate on stacking fault energy [4] is preserved as before (Equation 4), and a value of A_c is evaluated as $\sim 9 \times 10^{12}$. The plot shown in Fig. 6 can be used to estimate the parameter (Γ/Gb) provided that the alloy is showing dislocation climb control ($n \sim 5$) under the applied experimental conditions (stress and temperature).

To evaluate (Γ/Gb) for Al–1 wt% Cu alloy, the parameter $(\dot{\varepsilon}kT/D_cGb)/(\sigma/G)^5$ is calculated using the following data: shear modulus for the alloy is taken as that for aluminium ($3.022 \times 10^4 - 16T$ MPa), the diffusion coefficients are $D_{Al} = 6 \times 10^{-8} \exp(-101 \times 10^3/8.31T) m^2 s^{-1}$ [43] and $D_{Cu} = 6.5 \times 10^{-5} \exp(-135 \times 10^3/8.31T) m^2 s^{-1}$ [44]. The (Γ/Gb) value of the alloy inferred from Fig. 6 is ~ 0.026, which corresponds to Γ value of 190 mJ m^{-2}. This value of Γ is comparable with those estimated for other aluminium alloys Al–0.86 at % Cu (180 mJ m^{-2}) [24] and Al–10 at % Zn (150 mJ m^{-2}) [15]. [15].

Using the Weertman analysis [6, 7] for viscous glide in solid solutions based on the Cottrell–Jaswon interaction mechanism [34], the constant B in Equation 4 is calculated to have a value of $\sim 3 \times 10^{13}$. This value is slightly higher than that calculated previously [4, 37].

Equation 4 is depicted graphically in Fig. 7 by plotting $(1/X_B)(kT/eGb^3)^2$ versus $(\Gamma/Gb)^3(D_c/D_g)(\sigma/G)^2$ on a logarithmic scale. In this plot, Equation 4 is represented by a solid line having a slope of unity. The position of the line depends on the value of B. The data for Al–1 wt% Cu along with two Al–Cu alloys [24, 25] and three Al–Mg alloys [21] are superimposed on the figure, where the horizontal lines represent the stress ranges which are covered. The transition stress between the climb region and viscous glide region is represented by a solid circle on the horizontal line. It is clear that the data for Al–1 wt% Cu lie in the climb region. The transition stress for the other two Al–Cu alloys are in good agreement with prediction of Equation 4. For Al–Mg alloys, the parameter (Γ/Gb) is determined from Fig. 6, following the above-mentioned procedure using the diffusivities as $D_{Al} = 1.71 \times 10^{-4} \exp(-142 \times 10^3/8.31T) m^2 s^{-1}$ [26] and $D_{Mg} = 1.24 \times 10^{-4} \exp(-130 \times 10^3/8.31T) m^2 s^{-1}$ [45]. As listed in Table I, the Γ values for Al–Mg alloys are in reasonable agreement with the published values of Γ [46]. In addition, the value

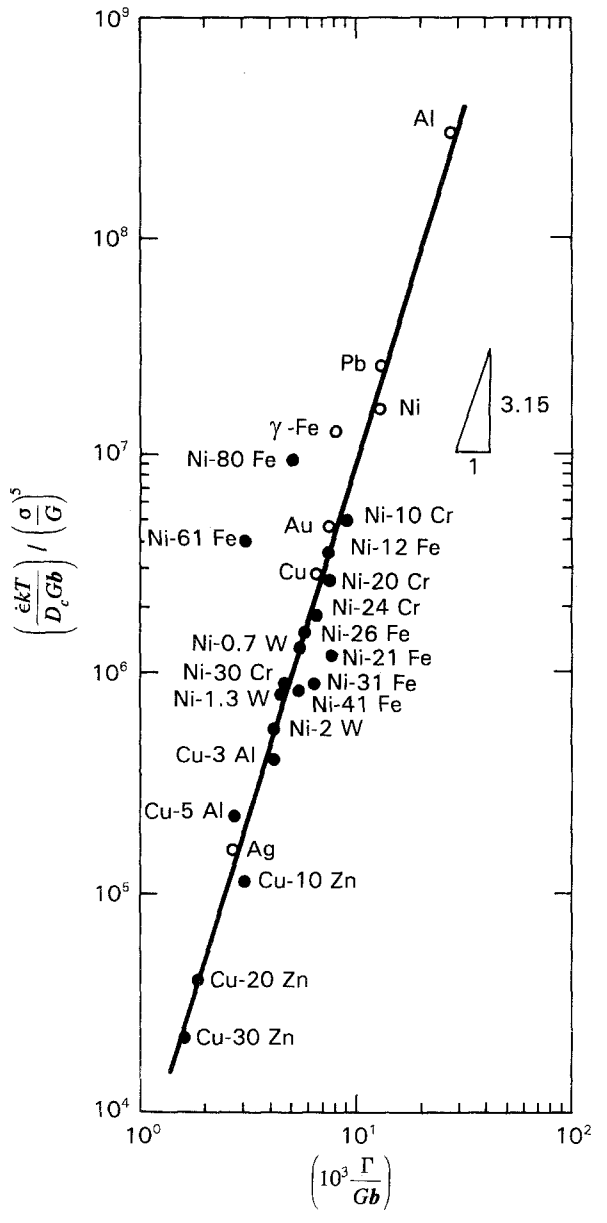

Figure 6 The stacking fault energy dependence of the normalized steady-state creep rate for a number of fcc pure metals and metal-class solid solutions.

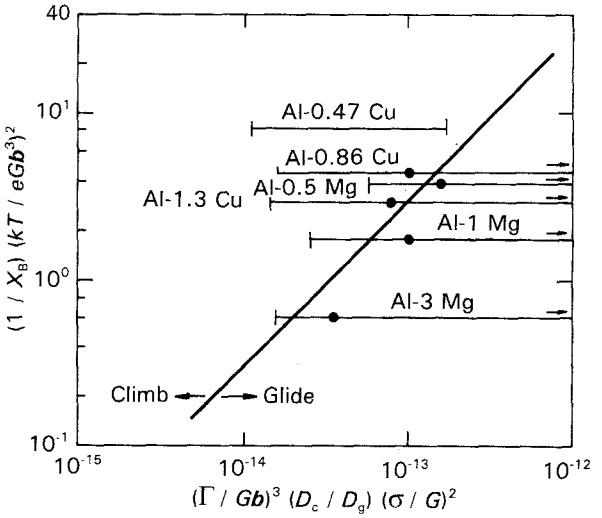

Figure 7 The climb–viscous glide criterion plotted logarithmically as $(1/X_B)(kT/eGb^3)^2$ versus $(\Gamma/Gb)^3(D_c/D_g)(\sigma/G)^2$ for $B = 3 \times 10^{13}$ and superimposed on the creep data of Al–0.47 at % Cu along with the data for other Al–Cu alloys [24, 25] and Al–Mg alloys [21]. (●) On the horizontal lines represent the transition stress from climb ($n \sim 5$) to viscous glide ($n \sim 3$).

TABLE I Stacking fault energy for Al–Mg alloys[a]

Alloy	T (K)	Γ/Gb	Γ (mJ m^{-2})
Al–0.5 Mg	600	0.0140	102
Al–1.1 Mg	600	0.0120	87
Al–3.25 Mg	600	0.0075	54

[a] Γ is calculated based on the shear modulus value of aluminium at room temperature.

for (D_c/D_g) for Al–Mg alloys is taken as unity; Weertman model is in agreement with the creep rates of Al–Mg alloys when D_g is taken equal to the aluminium diffusivity [47], i.e. $D_c \sim D_g$. The agreement is within a factor of 2 between the transition stress in Al–Mg alloys and the prediction of Equation 4 (see Fig. 7).

5. Conclusions

The creep characteristics of Al–1 wt% Cu studied at 813 K ($\sim 0.9\,T_m$) and over a stress range of 0.5–5 MPa suggest the following conclusions.

1. The stress exponent of 4.4, the shape of transient creep, and the activation energy for creep indicate that the creep behaviour of the alloy is dislocation climb controlled at high stresses.

2. At low stresses, the occurrence of dynamic recrystallization resulted in an increase in the stress exponent.

3. The stacking fault energy of any alloy can be estimated provided that the alloy shows dislocation climb control of creep behaviour under the experimental conditions. The Γ value for the present alloy is estimated to be 190 mJ m^{-2}.

4. The criterion for viscous glide–dislocation climb transition in solid solutions can predict the creep behaviour of an alloy provided that accurate values for the alloy parameters such as stacking fault energy, and climb and glide diffusivities are used in the analysis.

Acknowledgements

This work was supported by the Research Center, College of Engineering, King Saud University under Project no. 405/6. Thanks are extended to A. Choudhry for typing the manuscript.

References

1. J. WEERTMAN, *Trans. ASM* **61** (1968) 681.
2. J. E. BIRD, A. K. MUKHERJEE, and J. E. DORN, "Correlations between high-temperature creep behaviour and structure", Rep. No. UCRL-19056, Lawrence Radiation Laboratory, University of California, Berkeley, 1969.
3. O. D. SHERBY and P. M. BURKE, *Prog. Mater. Sci.* **13** (1967) 1325.
4. F. A. MOHAMED and T. G. LANGDON, *Acta Metall.* **22** (1974) 779.
5. J. WEERTMAN, *J. Appl. Phys.* **28** (1957) 362.
6. *Idem, ibid.* **28** (1957) 1185.
7. *Idem, Trans. AIME* **218** (1960) 207.
8. W. R. CANNON and O. D. SHERBY, *Metall. Trans.* **1** (1970) 1030.
9. K. L. MURTY, F. A. MOHAMED and J. E. DORN, *Acta Metall.* **20** (1972) 1009.
10. F. A. MOHAMED, *Metall. Trans.* **A9** (1978) 1013.
11. H. OIKAWA, K. SUGAWARA and S. KARASHIMA, *Trans. Jpn. Inst. Met.* **19** (1978) 611.
12. M. PAHUTOVA and J. CADEK, *Phys. Status Solidi A* **56** (1979) 305.
13. P. YAVARI, F. A. MOHAMED, and T. G. LANGDON, *Acta Metall.* **29** (1981) 1495.
14. M. S. SOLIMAN and F. A. MOHAMED, *Mater. Sci. Eng.* **55** (1982) 111.
15. *Idem, Metall. Trans.* **A15** (1984) 1893.
16. F. A. MOHAMED and Y. KIM, *Scripta Metall.* **11** (1977) 879.
17. H. OIKAWA, *ibid.* **12** (1978) 283.
18. T. FANG, R. RAO KILA, and K. L. MURTY, *Metall. Trans.* **A17** (1986) 1447.
19. J. S. WANG and W. D. NIX, *Acta Metall.* **34** (1986) 545.
20. M. S. SOLIMAN, *Mater. Sci. Eng.* **A112** (1989) 21.
21. H. OIKAWA, K. HONDA and S. ITO, *ibid.* **64** (1984) 237.
22. H. OIKAWA, H. SATO and K. MARUYAMA, *ibid.* **75** (1985) 21.
23. H. SATO and H. OIKAWA, *Scripta Metall.* **22** (1988) 87.
24. P. CHAUDHURY and F. A. MOHAMED, *Mater. Sci. Eng.* **A101** (1988) 13.
25. *Idem, Metall. Trans.* **A18** (1987) 2105.
26. T. S. LUNDY and J. F. MURDOCK, *J. Appl. Phys.* **33** (1962) 1671.
27. M. S. SOLIMAN, T. J. GINTER and F. A. MOHAMED, *Philos. Mag.* **A48** (1983) 63.
28. T. J. GINTER, M. S. SOLIMAN and F. A. MOHAMED, *ibid.* **A50** (1984) 9.
29. A. GOEL, T. J. GINTER and F. A. MOHAMED, *Metall. Trans.* **A14** (1983) 2309.
30. A. S. ARGON and S. TAKEUCHI, *Acta Metall.* **29** (1981) 1877.
31. S. TAKEUCHI and A. S. ARGON, *J. Mater. Sci.* **11** (1976) 1542.
32. W. R. JOHNSON, C. R. BARRETT and W. D. NIX, *Metall. Trans.* **A3** (1972) 963.
33. K. MONMA, H. SUTO and H. OIKAWA, *J. Jpn Inst. Met.* **28** (1964) 304.
34. A. H. COTTRELL and M. A. JASWON, *Proc. R. Soc. Lond. A* **199** (1949) 104.
35. F. A. MOHAMED, *Mater. Sci. Eng.* **61** (1983) 149.
36. R. FUENTES-SAMANIEGO and W. D. NIX, *Scripta Metall.* **15** (1981) 15.
37. M. S. SOLIMAN, *Res. Mechanica* **21** (1987) 155.
38. M. S. SOLIMAN and I. EL-GALALI, *J. Mater. Sci. Lett.* **7** (1988) 1027.
39. K. PARK, E. J. LAVERNIA and F. A. MOHAMED, *Acta Metall.* **38** (1990) 1837.
40. C. R. BARRETT and O. D. SHERBY, *Trans. AIME* **233** (1965) 1116.
41. R. M. BONESTEEL and O. D. SHERBY, *Acta Metall.* **14** (1966) 385.
42. F. A. MOHAMED and T. G. LANDGON, *J. Appl. Phys.* **45** (1974) 1965.
43. T. G. STOEBE, R. D. GULLIVER II, T. O. OGURTANI and R. HUGGINS, *Acta Metall.* **13** (1965) 701.
44. N. L. PETERSON and S. J. ROTHMAN, *Phys. Rev.* **B1** (1970) 3274.
45. S. J. ROTHMAN, N. L. PETERSON, I. J. NOWICKI and L. C. ROBINSON, *Phy. Status Solidi B* **63** (1974) K29.
46. P. DROPMANN, H. M. TENSI and H. BORCHERS, *Z. Metallkd.* **61** (1970) 848.
47. F. A. MOHAMED, *Mater. Sci. Eng.* **38** (1979) 73.

Received 28 May 1992
and accepted 7 January 1993